Heat and Momentum Transport Characteristics of Non-Newtonian Aqueous Thorium Oxide Suspensions

D. G. THOMAS

Oak Ridge National Laboratory, Oak Ridge, Tennessee

Heat transfer and pressure-drop measurements were made with non-Newtonian aqueous thorium oxide suspensions. A comparison of the results of the two different kinds of measurement allowed the general features of non-Newtonian thorium oxide suspension heat transfer to be readily identified, thus leading to a clear understanding of anomalies observed in previous suspension heat transfer studies.

Data were obtained at suspension concentrations up to 0.10 volume fraction solids, (1,000 g. of thorium/kg. of water) in systems having tube diameters of 0.318 and 1.030 in. In addition laminar-flow data were taken with a capillary-tube viscometer with a tube diameter of ⅛ in. and an *L/D* of 1,000. It was shown that laminar flow physical properties determined with the ⅛ in. diameter tube were satisfactory for correlating data taken with tubes up to 1.030 in. in diameter.

Until the present study information was not available which would permit a choice between two different viscosities for use in correlating non-Newtonian turbulent heat transfer and flow data. The limiting viscosity at very high shear rates is shown to give a unique correlation of turbulent data for tube diameters from 0.124 to 1.030 in., whereas the use of the effective viscosity (that is the viscosity evaluated at the point value of the wall shear stress corresponding to each given flow condition) gives a pronounced diameter effect in turbulent-flow correlations.

The data show that the onset of turbulence for both the pressure-drop and heat transfer measurements occurs at the same Reynolds number and is approximated by the value predicted by the Hedstrom criterion (*11*). The heat transfer transition region extends to Reynolds numbers a factor of four times greater than the critical, as is also the case with Newtonian materials. Heat transfer to thorium oxide slurries in fully developed turbulent flow is the same as that predicted by the usual correlations for Newtonian fluids to within the precision of the experimental data, provided that the Reynolds and Prandtl numbers are calculated with the limiting viscosity at high rates of shear, η, for this viscosity. An approximate form of Martinelli's momentum heat transfer analogy correlates the experimental results within +17 and −36%.

The form of thorium for use in an aqueous homogeneous power reactor is largely restricted to suspensions of thorium oxide in water (slurries) because of solubility, radiation and thermal stability, and nuclear cross-section considerations (*13*). Economic studies show that optimum thorium oxide concentrations should be 0.01 to 0.03 volume fraction solids in core and 0.075 to 0.125 volume fraction solids in blanket regions in such reactors. Since exploratory heat transfer measurements (*16*) with thorium oxide slurries in those concentration ranges showed marked deviations from usual Newtonian-fluid correlations at Reynolds numbers as large as 10^5, studies were initiated to determine the heat transfer and fluid-flow properties of thorium oxide slurries under turbulent-flow conditions.

It was the object of this investigation to:

1. Verify the suitability of the Sieder-Tate equation for correlating non-Newtonian suspension heat transfer coefficients at the higher Reynolds number.
2. Determine the nature of the deviations from the predicted *j* factors at the lower values of the Reynolds number.
3. Determine the most suitable experimental viscosity to use in the correlations.
4. Determine isothermal turbulent flow friction factors in the same equipment used to measure heat transfer coefficients.
5. Test applicability of heat and momentum transfer analogies for use with suspension data.

FLOW CHARACTERISTICS OF SUSPENSIONS

Although non-Newtonian technology has been thoroughly covered in several different review articles (*1, 15, 19, 30*), a brief discussion of some factors important in the laminar flow of non-Newtonian fluids will be given as background for the experimental results. Particular attention will be given to the definition of several different non-Newtonian viscosity terms:

1. The apparent viscosity is the viscosity at any given value of the rate of shearing strain [Eq. (1)].
2. The effective viscosity is the viscosity corresponding to the particular value of the wall shear stress under a given flow condition. The effective viscosity and apparent viscosity are equal for Newtonian fluids and are related by the Mooney-Rabinowitsch equation (*19*) when the fluids are non-Newtonian.
3. The limiting viscosity at high rates of shear is the asymptotic value of the viscosity below which the effective viscosity can never be reduced, a value always greater than the viscosity of the suspending medium. This definition applies to a large class of materials, including thorium oxide-water suspensions, which become more fluid as the shear rate is increased.

Aqueous thorium oxide slurries often have non-Newtonian laminar flow characteristics distinguished by a nonconstant relationship between the rate of shearing strain, *du/dr*, and the shear stress. Typical data are represented as a true shear diagram by the curve *ABCDEF* in Figure 1. At high rates of

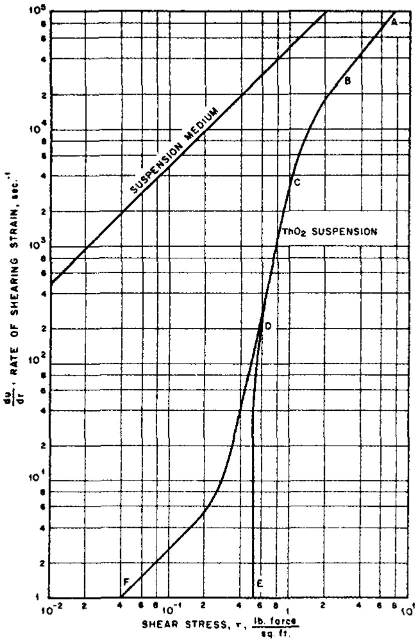

Fig. 1. Typical laminar flow shear diagram for thorium oxide suspension.

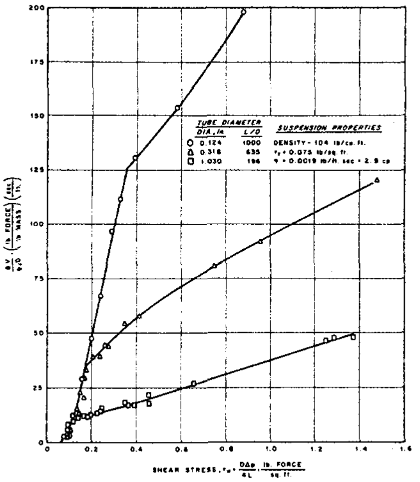

Fig. 2. Pseudo-shear diagram for thorium oxide slurry showing agreement of data taken in the laminar range with tubes of different diameters.

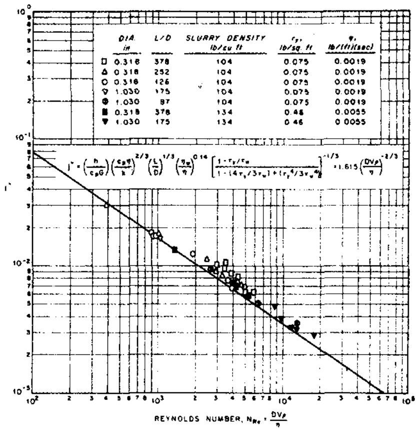

Fig. 3. Laminar heat transfer characteristics of thorium oxide slurries compared with theoretical equation.

shear the slurry curve (region AB) approaches but never crosses the curve for the suspending medium. At lower rates of shear the slurry curve (region BCD) deviates markedly from the curve for the suspending medium. At very low rates of shear the slurry data are observed in the region DEF with the data usually being closer to curve DE than to curve DF.

Although the determination of the relation between the laminar flow rate and pressure drop for flow in circular conduits is straightforward (*1, 4, 15, 19, 30*), an immediate difficulty in attempting to correlate nonlaminar flow non-Newtonian data is the need for a definition of the viscosity coefficient in Reynolds number. This is because the apparent viscosity

$$\mu_a = \frac{g_c \tau}{du/dr} \tag{1}$$

decreases from a large value at low rates of shear to a limiting value (region AB of Figure 1) at high rates of shear. Oldroyd (*24*) has proposed that the only viscosity coefficient which need be considered in turbulent flow (and in the laminar sublayer at the wall when the mainstream is turbulent) is the limiting value at high rates of shear. On the other hand it has also been suggested (*19*) that a suitable viscosity for use in calculation of the turbulent Reynolds number is the apparent viscosity determined at the particular value of the wall shear stress for each different flow condition. Although Equation (1) would give suitable values, it requires data for the shear stress as a function of the rate of shearing strain. However it is possible, by a redefinition of terms, to use capillary tube data directly (*19*). Laminar data taken with round tubes (*1, 15, 19*) are commonly plotted as $8V/g_cD$ vs. τ_w. The resultant plot is called a pseudo-shear diagram, and the term "effective" will be used to distinguish viscosities calculated from pseudo-shear diagrams from the apparent values calculated from true-shear diagrams; that is

$$\mu_e = \frac{\tau_w}{8V/g_cD} = \frac{D\Delta p/4L}{8V/g_cD} \tag{2}$$

A difficulty that arises in the practical application of Equation (2) for the determination of viscosities for use with turbulent flow data is that laminar flow must be obtained over the complete range of shear rates of interest. This can only be done with a viscometer having a tube diameter smaller than the tube diameter of the experimental equipment in which the turbulent flow data were taken. In fact the maximum value of the laminar shear rate which can be achieved with any given non-Newtonian fluid is roughly inversely proportional to the tube diameter. This introduces a complication in attempting to achieve high shear rates, particularly in dealing with suspensions, since several investigators (*17, 23*) have presented experimental evidence for a pronounced wall effect with small diameter capillary tubes. This effect is believed to be due to a layer of pure suspending medium adjacent to the wall which becomes significant as the diameter of the tube decreases toward the value of the effective particle diameter. This wall effect causes an underestimate to be made of the effective viscosity. In the present study it will be shown that there was no distinguishable wall effect with tubes having diameters from 0.124 to 1.030 in. for the thorium oxide suspensions used in the heat transfer studies. However a pronounced wall effect has been observed (*9*) with similar thorium oxide suspensions when the viscometer-tube diameter was 0.046 in. These results are consistent with previous experimental data (*17, 23*).

For convenience in comparing the effectiveness of different methods of correlation it is desirable to choose a rheological flow model to fit the laminar flow data. A suitable flow model should meet the following requirements:

1. It should fit the data sufficiently well at high shear rates so that accurate apparent viscosities can be calculated from the experimentally determined flow parameters.
2. It should extrapolate to give a limiting value of the viscosity at high rates of shear, that is greater than the viscosity of the suspending medium.

The model which was chosen in this investigation is the Bingham plastic model (*2*):

$$\frac{du}{dr} = \frac{g_c}{\eta}(\tau - \tau_y) \quad \text{for } \tau > \tau_y$$
$$\frac{du}{dr} = 0 \quad \text{for } \tau \leq \tau_y \tag{3}$$

It is recognized that there are some doubts as to the existence of a true yield stress as required by the Bingham plastic model and no claim is made that thorium oxide suspensions are Bingham plastics. However if Equation (3) fits the data adequately at the high shear rates observed at the wall in the present investigation, the problem of the existence of a true yield stress is relatively unimportant (*19*); that is the existence of an unsheared plug in the central region of the pipe as required by Equation (3) is unimportant as long as the laminar velocity profile is blunt and the velocity gradient

Table 1. Physical Property Variation of Thorium Oxide Slurries Used in Heat Transfer Tests

Test date	Number of heat transfer tests during interval	Temperature, °C.	Temperature, °F.	Slurry density, g./cc.	Slurry density, lb./cu. ft.	Coefficient of rigidity, η, centipoises	η, lb. mass/ft. sec.	η/μ_{H_2O}	Yield stress, τ, lb./sq. ft.
Aug. 1, 17, 23	76	27	81	1.69	105	3.1	0.0021	3.6	0.068
		50	122	1.70	106	2.6	0.0017	4.7	0.062
		80	176	1.64	102	2.0	0.0013	5.6	0.060
Sept. 19	51	27	81	1.67	104	3.5	0.0034	4.1	0.099
		50	122	1.67	104	2.9	0.0020	5.3	0.091
		80	176	1.67	104	2.0	0.0013	5.6	0.090
Jan. 17	28	24	75	2.11	132	8.2	0.0055	9.2	0.49
		54	129	2.03	127	5.7	0.0038	11.1	0.50
Feb. 6	20	26.5	80	2.11	132	5.4	0.0036	6.3	0.50
		56	133	2.08	130	4.5	0.0030	9.0	0.54
		74	165	2.05	128	4.0	0.0027	10.4	0.55
Mar. 11	14	23	73	2.01	125	5.2	0.0035	5.6	0.42
		50	122	2.00	125	4.6	0.0031	8.4	0.42
		70	158	2.01	125	3.1	0.0021	7.6	0.51

at the tube wall is predicted accurately.

In order to use the Bingham plastic model to calculate effective viscosities Equation (3) must be integrated (*3, 15*) for circular geometry, giving

$$8V/g_cD = 1/\eta\,[\tau_w - (4/3)\,\tau_y + (1/3)\,\tau_y^4/\tau_w^3] \qquad (4)$$

The effective viscosity for conditions where τ_w is large compared with τ_y can be obtained from Equation (4) by neglecting the last term on the right; the result is

$$\mu_e = \eta[1 + (g_c\,\tau_y\,D/6\eta V)] \qquad (5)$$

For high rates of shear the limiting viscosity with the Bingham plastic model used is simply η.

EQUIPMENT, PROCEDURE, AND CALIBRATION

Laminar flow rheological properties were determined with a horizontal tube viscometer made of stainless steel and a tube with 0.124-in. I.D. with $L/D = 1{,}000$. Measurements of laminar and turbulent flow heat transfer and isothermal pressure drop were made in a system in which the slurry was circulated with a pump, and the flow rate was measured with a weigh tank.

The horizontal-tube heat exchange section consisted of two copper tubes with inside diameters of 0.318 and 1.030 in. Periodic examination of the interior surface of the heat transfer tubes showed that there was no adhering film of slurry and that the tubes were bright and shiny. Measurements of isothermal laminar and turbulent flow pressure drop were made with the same tubes used in the heat transfer measurements. The static pressure taps were located 28 and 18 *L/D* downstream from the mixing pots of the ⅜- and 1⅛-in. tubes.

Heat Transfer Calculations

The rate of heat transfer was obtained from the rate of steam condensation in the transition and turbulent tests and from the axial temperature rise in laminar tests. The slurry side heat transfer coefficient was evaluated from the over-all heat transfer coefficient with the steam-and tube-wall resistance determined from periodic series of water calibration tests. The slurry heat capacity was considered to be an additive function of the heat capacities of the pure materials. The thermal conductivity of the slurry was calculated from the values for the pure material by the use of Maxwell's equation (*18*)

$$k_{sl} = k_{H_2O}\left[\frac{2k_{H_2O} + k_{ThO_2} - 2\phi\,(k_{H_2O} - k_{ThO_2})}{2k_{H_2O} + k_{ThO_2} + \phi\,(k_{H_2O} - k_{ThO_2})}\right] \qquad (6)$$

which is in good agreement with experimental data for thorium oxide suspensions (*12*). The thermal conductivity (*18*) of thorium oxide is 8.2 and 7.0 B.t.u./hr. ft. °F., and the specific heat (*18*) is 0.056 and 0.060 B.t.u./lb. °F. at 30° and 100°C. Typical values of slurry thermal conductivity at 50°C. are 0.45 and 0.50 B.t.u./hr. ft. °F. for slurries having volume fraction solids of 0.075 and 0.115, respectively. Typical values of slurry specific heat at 50°C. are 0.58 and 0.47 B.t.u./lb. °F. for slurries having volume fraction solids of 0.075 and 0.115, respectively.

Calibration of Equipment

Flow Tests with Water. Over 90% of the data for the three tubes fall within

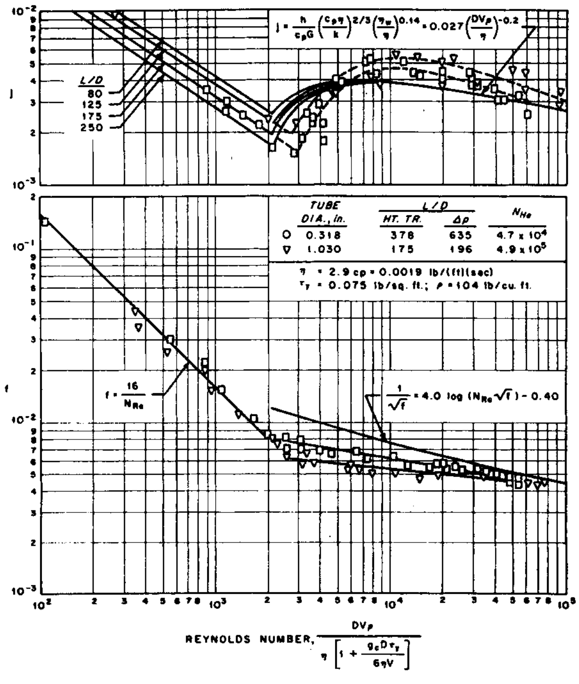

Fig. 4. Heat transfer and fluid flow characteristics of thorium oxide slurries showing an apparent diameter effect when one uses the effective viscosity to calculate Reynolds and Prandtl numbers.

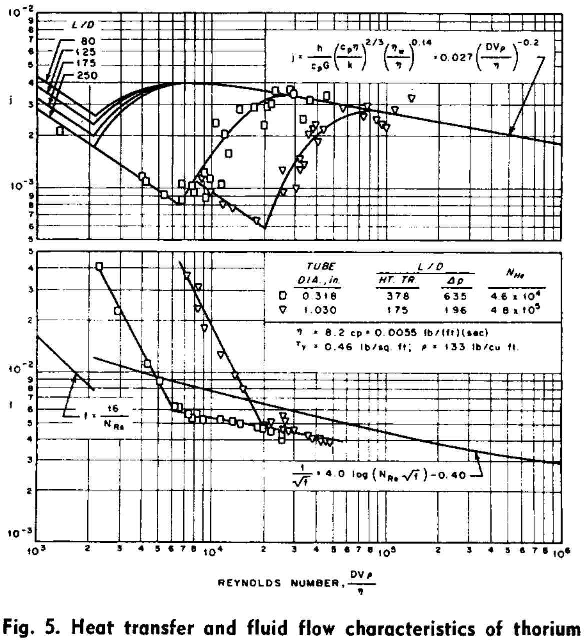

Fig. 5. Heat transfer and fluid flow characteristics of thorium oxide slurries with the limiting viscosity at high rates of shear used to calculate the Reynolds and Prandtl numbers.

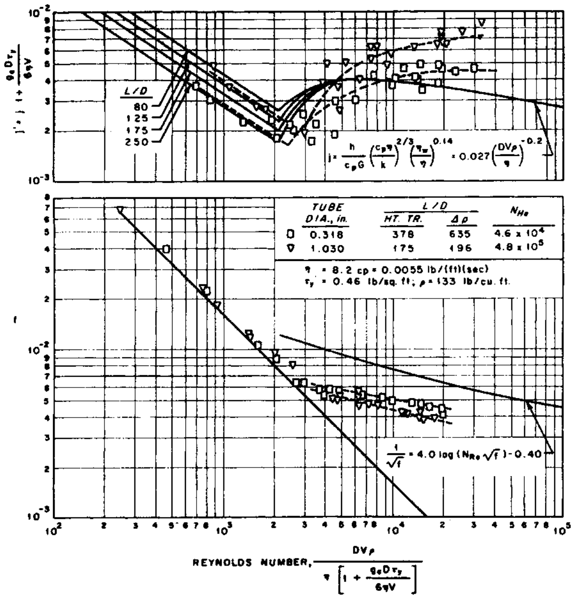

Fig. 6. Heat transfer and fluid flow characteristics of thorium oxide slurries showing an apparent diameter effect when one uses the effective viscosity to calculate Reynolds and Prandtl numbers.

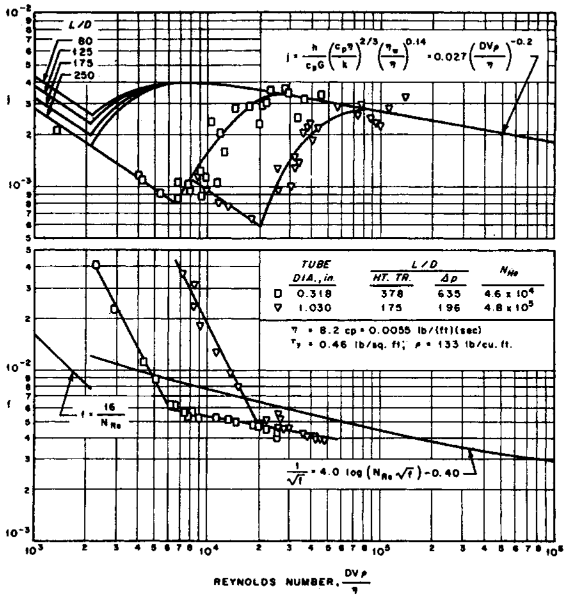

Fig. 7. Heat transfer and fluid flow characteristics of thorium oxide slurries with the limiting viscosity at high rates of shear used to calculate the Reynolds and Prandtl numbers.

±10% of the line given by the Nikuradse equation (*14*)

$$1/\sqrt{f} = 4.0 \log (N_{Re} \sqrt{f}) - 0.40 \quad (7)$$

over the Reynolds number range of 3,000 to 10^6, and there was no apparent trend with tube diameter. Laminar flow data taken with the smallest diameter tube agree to better than 5% with the laminar flow equation

$$f = 16/N_{Re} \quad (8)$$

Heat-Transfer Calibration Tests with Water. Turbulent flow heat transfer data taken with water in the two different tubes in the heat transfer system were in good agreement with the Sieder-Tate relationship (*29*)

$$\frac{h}{c_pG} = 0.027\, N_{Re}^{-0.2}\, N_{Pr}^{-2/3}\, (\mu/\mu_w)^{0.14} \quad (9)$$

with a mean deviation of ±10%. There appeared to be no trend with either tube diameter or L/D; however there was a tendency for the data to scatter slightly below the line. Heat balances, expressed as the ratio of q from condensate to q from axial temperature rise, averaged 0.992 for fifty-seven water-calibration tests, and 95% of the values were within ±5% of the average over a Reynolds number range from 10^4 to 6×10^5. The heat balance for 189 slurry tests averaged 1.01; 95% of the tests in which there was fully developed turbulent flow had heat balances falling within ±11% of the average, and heat balances for all 189 tests were within ±24% of the average.

LAMINAR FLOW THORIUM OXIDE SUSPENSION PROPERTIES

Comparison of laminar flow slurry pressure-drop measurements made with different systems is shown in Figure 2. The good agreement of laminar flow data taken with tubes having diameters of 0.124, 0.138, and 1.030 in. proves that wall effects are not important for the suspensions used in this study. The curves branching off from laminar into nonlaminar flow show the characteristic decrease in critical value of $8V/g_cD$ as the tube diameter increases. The laminar data for the three tubes are in good agreement internally and, except for the lowest values, follow a straight line relationship over the entire range in accord with the Buckingham equation [Equation (4)], giving a yield stress of 0.075 lb./sq. ft. and a coefficient of rigidity of 2.9 centipoises. Therefore the physical properties determined with the capillary-tube viscometer were considered to be satisfactory and were used in all of the following correlations. Flow properties as a function of temperature, determined through the course of the heat transfer tests, are given in Table 1. Both the yield stress and coefficient of rigidity varied during the tests in a more or less random manner. This variation of physical properties with time was partially taken into account by assuming a linear variation of coefficient of rigidity with time and using a mean value in Reynolds and Prandtl number calculations. No attempt was made to correct for variation of yield stress with time.

LAMINAR FLOW SUSPENSION HEAT TRANSFER

The present data are the first non-Newtonian suspension laminar flow

TABLE 2. RATIO OF EFFECTIVE VISCOSITY [(EQUATION 5)] TO LIMITING VISCOSITY AT HIGH RATES OF SHEAR FOR RANGE OF FLOW CONDITIONS ATTAINED IN HEAT TRANSFER STUDY WITH THORIUM OXIDE SLURRY; $\tau_y = 0.075$ lb./sq. ft.; $\eta = 0.00195$ lb./(ft.)(sec.)

	Tube dia., in.	Velocity, ft./sec.	Reynolds number $DV\rho/\mu_e$	Reynolds number $DV\rho/\eta$	μ_e/η
1. Lowest flow rate attained in heat transfer experiment	0.318	0.25	0.17×10^2	3.87×10^2	22.2
	1.030	0.26	0.13×10^2	1.04×10^3	80.0
2. Transition from laminar flow*	0.318	3.9	2.28×10^3	5.50×10^3	2.41
	1.030	3.7	2.76×10^3	1.60×10^4	5.80
3. $(DV\rho/\eta) = 4(DV\rho/\eta)_{\text{crit.}}$*	0.318	15.6	1.60×10^4	2.20×10^4	1.35
	1.030	14.8	2.90×10^4	6.40×10^4	2.20
4. Highest flow rate attained in heat transfer experiment	0.318	47.0	6.16×10^4	6.85×10^4	1.11
	1.030	30.9	9.3×10^4	1.58×10^5	1.70

* Values taken from smoothed curves of data.

heat transfer data that have been published which afford a check of theoretical equations. Hirai (*10*) has presented a theoretical analysis of laminar heat transfer of a Bingham plastic fluid and has shown that the equation

$$\left(\frac{h}{c_pG}\right)\left(\frac{c_p\eta}{k}\right)^{2/3}\left(\frac{\eta_w}{\eta}\right)^{0.14}\left(\frac{L}{D}\right)^{1/3}\left[\frac{1-\tau_y/\tau_w}{1-(4\tau_y/3\tau_w)+\tau_y^4/3\tau_w^4}\right]^{1/3} = 1.615\left(\frac{DV\rho}{\eta}\right)^{-2/3} \qquad (10)$$

is a valid approximation provided the Nusselt number, (hD/k), is greater than 8.1.

Laminar flow heat transfer data for two different thorium oxide slurries having volume fraction solids of 0.075 and 0.12 in two different tubes with heated length L/D ratios from 87 to 378 are plotted in Figure 3. The agreement of the data with the theoretical expression is quite satisfactory, the mean value for the data is 11% above the theoretical line, and 95% of the data fall within a band of ±15% over a Reynolds number (DV_ρ/η) range from 400 to 18,000. The point at Reynolds number 387 had a Nusselt number of 5.9; all other data had Nusselt numbers greater than 8.3, thus meeting the requirement given by Hairi for the use of Equation (10). The value of the Sieder-Tate (*29*) correction factor $(\eta_w/\eta)^{0.14}$ was always greater than 0.88. The difference in value of the Sieder-Tate correction with the two viscosities, μ_e [Equation (5)] and η, at the same flow conditions was never more than 8%; therefore the more convenient limiting viscosity at high rates of shear was chosen for use in subsequent correlations.

HEAT TRANSFER AND FLOW CHARACTERISTICS OF SUSPENSIONS IN THE TRANSITION AND TURBULENT FLOW REGION

Friction-factor and heat transfer data taken with the same slurry are shown in Figures 4 and 5 as a function of Reynolds number. The Reynolds numbers were calculated by using the effective viscosity, μ_e [Equation (5)], and the limiting viscosity at very high shear, η respectively. There is a very good agreement in both figures between the laminar flow pressure-drop data for both the 0.318- and 1.030-in. diameter tubes and the theoretical laminar curves. The fact that two laminar flow curves are observed in Figure 5 results from the diameter term in the Hedstrom number (*11*), thus giving two different curves even though only one set of slurry properties is involved.

TABLE 3. RATIO OF EFFECTIVE VISCOSITY [EQUATION (5)] TO LIMITING VISCOSITY AT HIGH RATES OF SHEAR FOR RANGE OF FLOW CONDITIONS ATTAINED IN HEAT TRANSFER STUDY WITH THORIUM OXIDE SLURRY; $\tau_y = 0.46$ lb./sq. ft.; $\eta = 0.0055$ lb./(ft.)(sec.)

	Tube dia., in.	Velocity, ft./sec.	Reynolds number $\frac{DV\rho}{\mu_e}$	Reynolds number $\frac{DV\rho}{\eta}$	$\frac{\mu_e}{\eta}$
1. Lowest flow rate attained in heat transfer experiment	0.318	1.27	0.84×10^2	1.33×10^3	15.90
	1.030	4.50	8.66×10^2	8.56×10^3	9.89
2. Transition from laminar flow*	0.318	9.8	1.7×10^3	6.1×10^3	3.6
	1.030	10.4	3.3×10^3	2.0×10^4	6.0
3. $\frac{DV\rho}{\eta} = 4\left(\frac{DV\rho}{\eta}\right)_{crit.}$*	0.318	29.0	1.4×10^4	2.4×10^4	1.7
	1.030	23.0	1.9×10^4	8.0×10^4	4.3
4. Highest flow rate attained in heat transfer experiment	0.318	43.1	3.02×10^4	4.51×10^4	1.49
	1.030	32.7	3.39×10^4	1.37×10^5	4.04

* Values taken from smoothed curves of data.

Since the laminar flow properties used in the calculation of the Reynolds and Hedstrom numbers for the 0.318- and 1.030-in. diameter tube were determined from data taken with the 0.124-in. diameter tube, the good agreement of the data with the theoretical laminar flow lines in Figures 4 and 5 substantiates the observation that there is no significant laminar wall effect with thorium oxide slurries for flow in tubes in the diameter range 0.124 to 1.030 in.

Examination of the transition and turbulent flow data for heat transfer and fluid flow plotted in Figure 4, in which the effective viscosity was used in the calculation of the Reynolds and Prandtl numbers, shows that the transition from laminar flow occurs in the Reynolds number range 2,000 to 3,000, as expected (*19*). However both the heat transfer and the fluid flow data show a pronounced diameter effect in the turbulent region. This is a direct result of the fact that the effective viscosity is a function of tube diameter. (This is true for any model chosen to represent the laminar flow data and is not a characteristic of the particular model chosen for this study.) This is shown in Table 2 which gives the ratio of the effective viscosity [Equation (5)] to limiting viscosity at high rates of shear for the range of flow conditions attained in the heat transfer study. The ratio of effective viscosities for different tube diameters under similar flow conditions decreases from 2.45 at a value of DV_ρ/μ_e of 3×10^2 to 1.70 at a value of DV_ρ/μ_e of 6×10^4. Hence although the effective viscosity is suit-

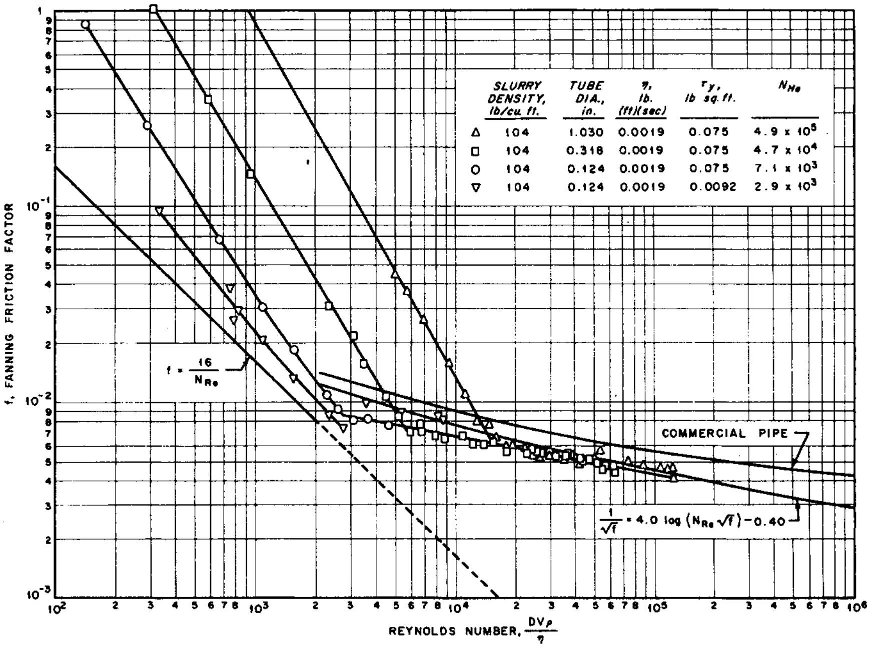

Fig. 8. Friction factor-Reynolds number plot for aqueous thorium oxide slurries showing agreement of data taken in the turbulent range with tubes of different diameters.

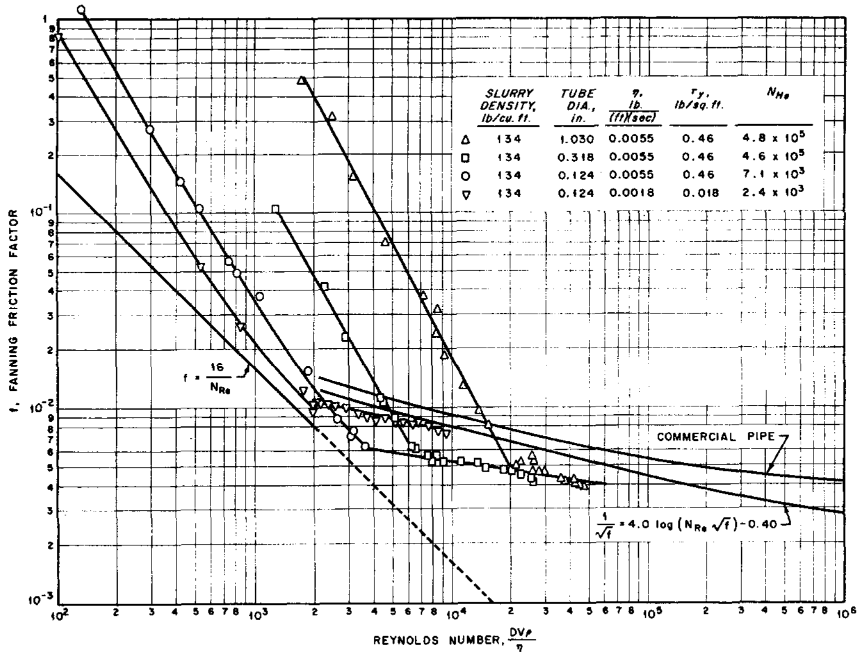

Fig. 9. Friction factor-Reynolds number plot for aqueous thorium oxide slurries showing agreement of data taken in the turbulent range with tubes of different diameter.

able for transposing the data to give a critical Reynolds number in the range 2,000 to 3,000, it does not appear to meet the additional requirement of uniquely correlating the data for a particular suspension, independent of tube diameter.

This table also shows that, depending on the tube diameter, the ratio of effective to limiting viscosity was reduced from 80 to 1.7 in going from the lowest to the highest flow rates, and even at the highest flow rates attained the effective viscosity was 10 to 70% greater than the limiting viscosity at high rates of shear provided that the coefficient of rigidity adequately represents the limiting viscosity. Hence even at the high flow rates the slurry possessed appreciable non-Newtonian characteristics.

It is of interest to note from Table 2 that the critical velocity for transition from laminar flow is almost independent of tube diameter. It has been pointed out previously that the critical velocity for materials approximated by the Bingham plastic relation is primarily a function of yield stress and is only a very weak function of the tube diameter and coefficient of rigidity (*31*).

Examination of the data plotted in Figure 5, in which the limiting viscosity at high shear rates is used in the calculation of the Reynolds and Prandtl numbers, shows the characteristic displacement of the laminar data with tube diameter corresponding to the different values of the Hedstrom number (*11*). The heat transfer and the fluid flow data having the same Hedstrom number show the transition from laminar flow at the same Reynolds number. The heat transfer data for both tube diameters are correlated by the conventional Newtonian line given by Equation (9), provided that the Reynolds number is 3 to 5 times the critical value for the onset of nonlaminar flow. The nonlaminar friction factor data for both tube diameters are correlated by a single line. The slurry friction factors are below the smooth-tube line for Newtonian fluids, given by Equation (7), but tend to approach this line at higher Reynolds numbers.

Friction factor and heat transfer data taken with a more concentrated (and hence more non-Newtonian) suspension are shown in Figures 6 and 7 and Table 3. These results are completely consistent with the data and discussion given above. Additional tests in which the L/D ratios of the heated sections were 126 and 252 for the ⅜-in. tube and 87 for the 1-⅛-in. tube were also in good agreement with these data.

The experimental results given in Figures 5 and 7 show that, for the range of variables covered, turbulent heat transfer and pressure-drop data for a given suspension can be correlated uniquely, independent of tube diameter, provided the experimentally determined limiting viscosity at high shear rates is used in calculating the Reynolds and Prandtl numbers. In addition it is apparent that the deviations observed at lower Reynolds numbers in previous studies were associated with the transition from turbulent to laminar flow. The slurry heat transfer transition data cover a range of Reynolds numbers from 3 to 5 times the value of the critical Reynolds number for the laminar-nonlaminar transition. This corresponds very closely to the range covered by Newtonian fluids, and in fact, except for the displacement in critical Reynolds numbers due to the non-Newtonian laminar characteristics of the slurry, the thorium oxide suspension heat transfer data are very similar in appearance to Newtonian heat transfer data.

TURBULENT FLOW CHARACTERISTICS OF SUSPENSIONS

In order to determine whether the deviation of the turbulent flow data from the Newtonian curve was due merely to the suspended solids or to the non-Newtonian characteristics of the mixture, sodium silicate was added to the suspension to reduce the yield stress, and the flow characteristics were redetermined with the 0.124-in. diameter viscometer tube. The results are shown on Figures 8 and 9, and the before and after data (slurry 5 and 2) are included in Table 4. As can be seen, the addition of silicate reduced the non-Newtonian characteristics, and at the same time the turbulent flow friction factors were increased toward the smooth-tube Newtonian friction-factor curve. Although this is not conclusive proof, it indicates that the flow deviations are truly the result of the non-Newtonian characteristics.

TABLE 4. FLOW PROPERTIES OF THORIUM OXIDE SLURRIES

	Slurry density, g./cc.	Slurry density, lb./cu. ft.	Laminar Flow Constants: Coefficient of rigidity, η, centipoise	Coefficient of rigidity, η, lb./ft. sec.	Yield stress, τ_y, lb./sq. ft.	Blasius constants $f = B_1 N_{Re}^{-b}$: B_1	b
1	1.25	95	2.3	0.0015	0.013	0.0497	0.211
2*	2.08	130	2.7	0.0018	0.018	0.057	0.220
3	1.67	104	2.9	0.0020	0.075	0.0398	0.192
4	2.02	126	5.2	0.0035	0.34	0.0327	0.180
5	2.14	133	8.2	0.0055	0.46	0.0239	0.164

* Sodium silicate added to slurry 5 to decrease non-Newtonian characteristics.

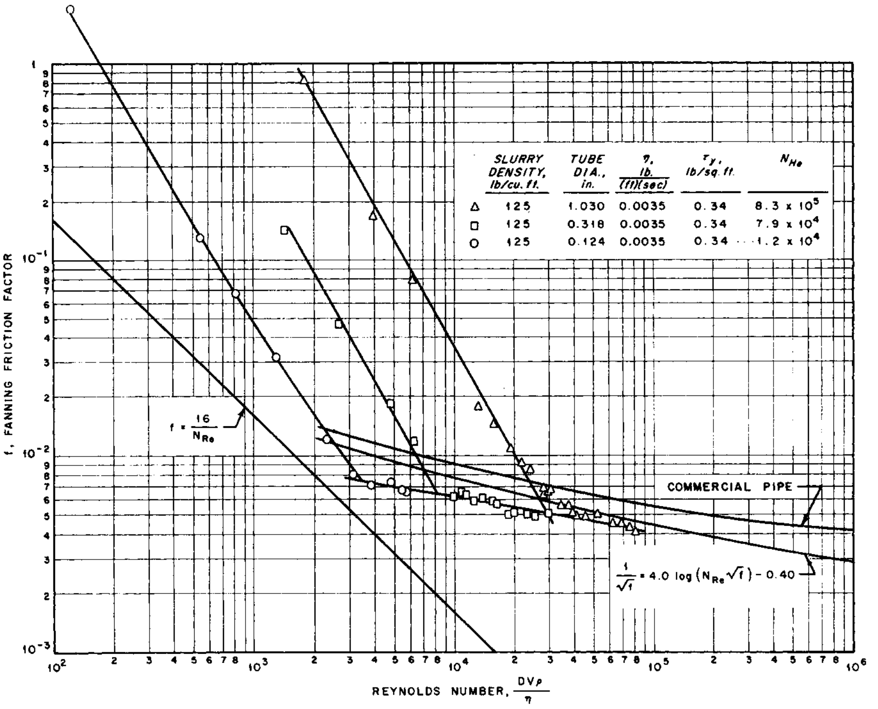

Fig. 10. Friction factor-Reynolds number plot for aqueous thorium oxide slurries showing agreement of data taken in the turbulent range with tubes of different diameters.

The data for concentrated slurries, shown in Figures 8 to 10, were obtained with tubes having diameters from 0.124 to 1.030 in. For any particular slurry the turbulent flow data obtained with the three different tubes are correlated by a single straight line. As a result it is concluded that there is no turbulent flow tube-diameter effect with thorium oxide suspensions for tubes having diameters in the range 0.124 to 1.030 in. provided the limiting viscosity at high rates of shear is used in the Reynolds number calculation.

The turbulent flow data for both treated and untreated slurries may be correlated with the Blasius (*14*) relationship

$$f = B_1 N_{Re}^{-b} \tag{11}$$

provided that the coefficients are given as functions of the laminar non-Newtonian characteristics. The values of the coefficient and exponent for the different slurries are given in Table 4. These data are fitted by the expressions

$$B_1 = 0.079 \left(\frac{\mu}{\eta}\right)^{0.48} \tag{12}$$

and

$$b = 0.25 \left(\frac{\mu}{\eta}\right)^{0.15} \tag{13}$$

which reduce to the usual Newtonian values as the coefficient of rigidity becomes equal to the coefficient of viscosity of the suspending medium.

Although no velocity profiles were measured, it may be instructive to calculate velocity profiles following arguments (*22*) proposed independently by Prandtl and von Karman (*32*). They suggested a method of relating an empirical equation for the velocity distribution

$$\frac{u}{U} = \left(\frac{y}{R}\right)^{1/m} \tag{14}$$

to Blasius' law for friction loss [Equation (11)] and obtained an expression for the value of the velocity-distribution exponent in terms of the exponent on the Reynolds number in the friction-factor equation

$$m = \frac{2-b}{b} \tag{15}$$

A log-log plot of the velocity-distribution exponent and the yield stress obtained from the data of Table 2 gives a straight line. Yield stresses corresponding to different power-law exponents obtained from this line are

$\left(\frac{1}{m}\right)$ [See Equation (14)]	τ_y, (lb./sq. ft.)
1/7	0.003
1/8	0.015
1/9	0.055
1/10	0.200
1/11	0.55

For Newtonian fluids (*14*) the 1/7 power law gives good agreement with experimentally measured velocity profiles for Reynolds numbers up to 10^5.

The increase of bluntness of the velocity profile as the non-Newtonian characteristics are increased has been predicted previously (*7*) and is consistent with a damping effect of the yield stress on the turbulent velocity fluctuations in the central regions of the pipe. The damping of the turbulent fluctuations would be expected to have little effect on wall processes such as heat transfer and friction loss but could be very important in processes where diffusion in the central region of the pipe is important. Thus additional measurements are needed not only to determine the velocity profile but also to determine the nature and extent of the turbulent velocity fluctuations in suspensions which have non-Newtonian laminar flow characteristics. The only turbulent velocity profile measurements (*28*) on non-Newtonian systems have been made with organic solutions which may have had elastic characteristics (*7*), thus obviating their application to suspensions.

MOMENTUM HEAT TRANSFER ANALOGIES

The good agreement observed for heat transfer and pressure-drop data in turbulent flow with tubes of different diameter with the limiting viscosity at high rates of shear used to calculate

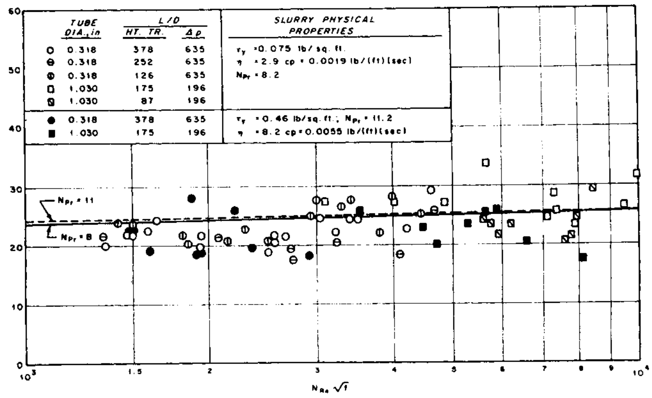

Fig. 11. Test of Martinelli's heat and momentum transfer analogy.

the Reynolds and Prandtl number makes it desirable to test the usefulness of momentum heat transfer analogies (*8, 14*) for correlating aqueous thorium oxide suspension data. It must be recognized that although all analogies become identical at a Prandtl number of unity (*16*), none are completely satisfactory for the complete Prandtl number range from 0.01 to 1,000 or greater. Liquid metal suspensions would fall in the former category, while non-Newtonian organic solutions often are in the latter (*20*). Selection of the most suitable analogy depends on the value of the Prandtl number. Since the Prandtl number in the present investigation is about 10, little difference would be expected in the application of the different analogies.

The data for fully developed turbulent flow were in substantial agreement with the Colburn, Prandtl, von Karman, Friend and Metzner and Martinelli analogies; the maximum deviation of the data from each of these analogies is given in Table 5. The best fit was observed with the Martinelli analogy, which was developed following von Karman's assumption of a buffer layer between the laminar sublayer and the turbulent core. Martinelli's analogy may be written as

$$j = \frac{\dfrac{\epsilon_H}{\epsilon_M}\sqrt{\dfrac{f}{2}}\;(N_{Pr})^{2/3}\;\dfrac{T_w - T_c}{T_w - T_b}}{5\left[\dfrac{\epsilon_H}{\epsilon_M} + \ln\left(1 + 5\dfrac{\epsilon_H}{\epsilon_M}N_{Pr}\right) + 0.5\,F_1 \ln \dfrac{N_{Re}}{60}\sqrt{\dfrac{f}{2}}\right]} \tag{16}$$

Values of F_1 have been tabulated (*14*) as a function of Reynolds and Peclet numbers, and for the present data F_1 values were between 0.99 and 1.00. Values of $(T_w - T_c)/(T_w - T_b)$ have been tabulated as a function of Reynolds and Prandtl numbers and for the present data were between 0.958 and 0.963. In the absence of experimental data the ratio ϵ_H/ϵ_M is commonly taken as unity. With these values the Martinelli equation reduces to

TABLE 5. COMPARISON OF DIFFERENT HEAT MOMENTUM TRANSFER ANALOGIES WITH EXPERIMENTAL DATA

Analogy	Reference	Deviation of data from predicted value, % Positive	Negative
Martinelli	*14*	17	36
Friend and Metzner	*8*	41	28
Prandtl	*14*	53	22
Colburn	*14*	3	50

$$\frac{\sqrt{f}}{j} = 2.120 \log N_{Re}\sqrt{f} + 17.48 \tag{16a}$$

for a Prandtl number of 8 and to

$$\frac{\sqrt{f}}{j} = 1.715 \log N_{Re}\sqrt{f} + 19.07 \tag{16b}$$

for a Prandtl number of 11. The friction-factor and the j-factor data for Reynolds numbers greater than 4 times the critical number from Figures 5 and 7 are plotted in Figure 11 as $\sqrt{f}/j$ vs. log $N_{Re}\sqrt{f}$. The Martinelli lines for the two different Prandtl numbers, Equations (*16a*) and (*16b*), are also included. All the turbulent flow, heat transfer, and pressure-drop data are included on a single plot and show reasonably good agreement with the Martinelli lines.

DESIGN PROCEDURE

The thorium oxide suspension heat transfer data shown in Figures 4 to 7 show a dip region at Reynolds numbers extending from the critical value for the transition to about $4(N_{Re})_c$. A similar dip region was first identified for Newtonian fluids by Colburn (*5*). Since the value of the critical velocity for the transition (4 to 10 ft./sec. for slurries with values of the yield stress from 0.075 to 0.5 lb./sq. ft.) is already approaching the range of velocities commonly used in heat exchanger design, a graphical procedure similar to the one originally proposed by Colburn (*5*) appears to be the most suitable method for avoiding the ambiguities associated with design for this dip region. The design procedure recommended is:

1. Calculate the value of the Hedstrom number, $N_{He} = g_c\rho\,\tau_y\,D^2/\eta^2$, and identify its location on a Fanning friction factor—Reynolds number (DV_ρ/η) plot containing the Hedstrom number grid as a parameter (Figure 12).
2. Locate the turbulent flow friction factor line on the same plot by the use of Equations (11), (12), and (13).
3. Calculate the laminar flow j-factor by the use of the value of the critical Reynolds number $(N_{Re})_c$ determined from the intersection of the laminar and turbulent flow lines obtained in steps 1 and 2 above. Plot the value calculated above on a Newtonian j-factor—Reynolds number plot, and locate the laminar heat transfer line from this point with a slope of $-2/3$.
4. Connect the laminar j-factor point at $(N_{Re})_c$ to the turbulent flow Newtonian j-factor curve at $N_{Re} = 4(N_{Re})_c$ with a smooth curve characteristic of the j-factor curve in the dip region.

This procedure completely identifies a j-factor curve from which heat transfer coefficients can be obtained for any particular suspension in the laminar, transition, and fully developed turbulent flow region. This procedure has been verified only for slurry temperatures below 100°C. and care should be used in applying it to systems at higher temperatures.

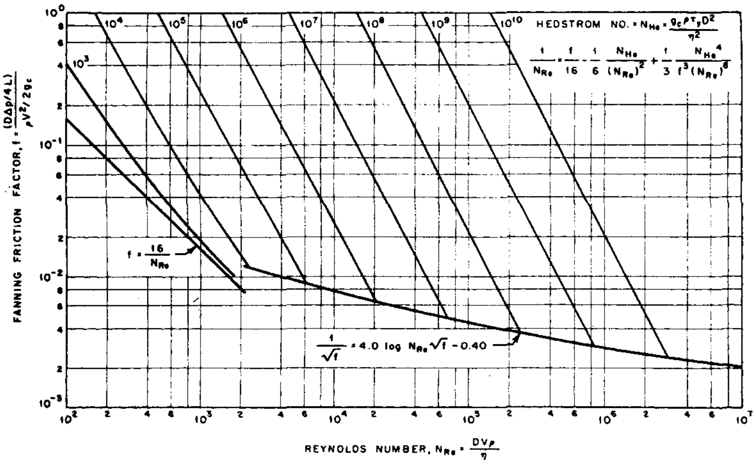

Fig. 12. Friction factor-Reynolds number diagram for laminar flow of Bingham plastic materials in round pipes.

CONCLUSIONS

The Sieder-Tate equation, or modifications thereof, has been shown to correlate non-Newtonian thorium oxide suspension heat transfer data satisfactorily provided that the data are taken at Reynolds numbers four times the value of the critical Reynolds number for the laminar transition. The limiting viscosity at high rates of shear has been identified as the correct experimental viscosity term for use in calculating turbulent flow Reynolds and Prandtl numbers for use in conventional j- and f-factor correlations. Previously observed deviations of the j-factor below the predicted values at Reynolds numbers as high as 20,000 to 100,000 were in all probability due to operation in the dip region, originally identified by Colburn as being associated with the laminar-transition region.

Although the nature of the nonlaminar flow of non-Newtonian slurries has not been unequivocally established, arguments based on heat and momentum transfer are consistent with the existence of fully developed turbulence at Reynolds numbers four times the critical Reynolds number. Nevertheless it is believed that the presence of particulate matter having sufficient particle-particle interaction to produce the observed yield stress makes a measurement of the extent of random velocity fluctuations necessary to demonstrate whether the observed nonlaminar results are due to turbulence similar to that existing in Newtonian fluids or to entirely different flow phenomena. This is particularly true in the central regions of the pipe, where the yield stress is greater than the shear stress and would be expected to damp the turbulent fluctuations.

ACKNOWLEDGMENT

Appreciation is expressed to Dr. R. N. Lyon for his support, suggestions, and criticism, and to Mr. P. H. Hayes for his capable assistance in taking data.

NOTATION

a = coefficient of velocity distribution equation
b = exponent of Blasius equation, dimensionless
B_1 = coefficient on Blasius equation, dimensionless
c_p = specific heat, B.t.u./(lb.) (°F.)
D = tube diameter, ft.
f = Fanning friction factor, dimensionless
g_c = conversion factor, (lb. mass/lb. force) (ft./sec.^{2})
G = mass flow rate, lb./(hr.) (sq. ft.)
h = film coefficient of heat transfer, B.t.u./(hr.) (sq.ft.) (°F.)
j = heat-transfer factor, dimensionless
k = thermal conductivity, B.t.u./(hr.) (sq. ft.) (°F./ft.)
k_{H_2O} = thermal conductivity of water, B.t.u./(hr.) (sq. ft.) (°F./ft.)
k_{sl} = thermal conductivity of slurry, B.t.u./(hr.) (sq. ft.) (°F./ft.)
k_{ThO_2} = thermal conductivity of thorium oxide, B.t.u./(hr.) (sq. ft.) (°F./ft.)
L = length, ft.
m = exponent in velocity-profile expression, dimensionless
N_{He} = Hedstrom number, $g_c \rho \tau_y D^2/\eta^2$, dimensionless
N_{Pr} = Prandtl number, $c_p \mu/k$, $c_p \mu_e/k$, or $c_p \eta/k$, dimensionless
N_{Re} = Reynolds number, $DV\rho/\mu$, $DV\rho/\mu_e$, or $DV\rho/\eta$, dimensionless
$(N_{Re})_c$ = critical Reynolds number for laminar transition, dimensionless
q = rate of heat transfer
R = tube radius, ft.
u = local fluid velocity, ft./sec.
U = maximum fluid velocity, ft./sec.
V = mean fluid velocity, ft./sec.
y = distance from pipe wall, ft.
du/dr = velocity gradient, sec.$^{-1}$
Δp = over-all pressure drop, lb./sq. ft.
Δt = difference between temperature of pipe wall and any point y, °F.
Δt_{max} = difference between temperature of pipe wall and center of pipe, °F.

Greek Letters

η = coefficient of rigidity, lb./ft. sec.
μ = viscosity at bulk mean temperature, lb./ft. sec.
μ_a = apparent viscosity, Equation (1), lb./ft. sec.
μ_e = effective viscosity, Equation (3), lb./ft. sec.
μ_w = viscosity at wall temperature, lb./ft. sec.
ρ = fluid density, lb./cu. ft.
τ = shear stress, lb./sq. ft.
τ_w = wall shear stress, $D\Delta p/4L$, lb./sq. ft.
τ_y = yield stress, lb./sq. ft.
ϕ = volume fraction solids, dimensionless

LITERATURE CITED

1. Alves, G. E., D. F. Boucher, and R. L. Pigford, *Chem. Eng. Progr.*, **48**, 385 (1952).
2. Bingham, E. C., "Fluidity and Plasticity," McGraw-Hill, New York (1922).
3. Buckingham, E., *Am. Soc. Testing Materials, Proc.*, **21**, 1154 (1921).
4. Christiansen, E. B., N. W. Ryan, and W. E. Stevens, *A.I.Ch.E. Journal*, **1**, 544 (1955).
5. Colburn, A. P., *Trans. Am. Inst. Chem. Engrs.*, **29**, 174 (1933).
6. de Waele, A., *J. Oil & Colour Chemists Assoc.*, **4**, 33 (1923).
7. Dodge, D. W., and A. B. Metzner, *A.I.Ch.E. Journal*, **5**, 189 (1959).
8. Friend, W. L., and A. B. Metzner, *ibid.*, **4**, 393 (1958).
9. Gibson, C. H., Personal communication (August, 1958).
10. Hirai, E., *Chem. Eng. (Japan)*, **21**, 17 (1957); *A.I.Ch.E.. Journal*, **5**, 130 (1959).
11. Hedstrom, B. O. A., *Ind. Eng. Chem.*, **44**, 561 (1952).
12. Johnson, F. A., "The Thermal Conductivity of Aqueous Thoria Suspensions," AERE R/R 2578 (June, 1958).
13. Kitzes, A. S., and R. N. Lyon, "Aqueous Uranium and Thorium Slurries," *Proc. of the International Conference on Peaceful Uses of Atomic Energy, Vol. 9, Reactor Technology and Chemical Processing*, United Nations Publishers, New York (1959).
14. Knudsen, J. G., and D. L. Katz, "Fluid Dynamics and Heat Transfer," McGraw-Hill, New York (1958).
15. Lapple, C. E., *et al.*, "Fluid and Particle Mechanics," Univ. Del., Newark (1954).
16. Lawson, C. G., in "Nuclear Engineering Handbook," H. Etherington, ed., pp. 13-78, McGraw-Hill, New York (1958).
17. Maude, A. D., and R. L. Whitmore, *Br. J. App. Phys.*, **7**, 98 (1956).
18. McBride, J. P., and D. G. Thomas, "Technology of Aqueous Suspensions," J. A. Lane, H. G. MacPherson, and F. Maslan, ed., chap. 4, Addison Wesley, Reading, Massachusetts (1958).
19. Metzner, A. B., in "Advances in Chemical Engineering," T. B. Drew and J. W. Hooper, Jr., ed., pp. 79-150, Academic Press, New York (1956).
20. ———, and P. S. Friend, *Ind. Eng. Chem.*, **51**, 879 (1959).
21. Metzner, A. B., D. A. Vaughn, and G. L. Houghton, *A.I.Ch.E. Journal*, **3**, 92 (1957).
22. Miller, Benjamin, *Trans. Am. Soc. Mech. Engrs.*, **71**, 347 (1949).
23. Mooney, Melvin, *J. Rheology*, **2**, 210 (1931).
24. Oldroyd, J. G., "Proc. Int. Rheological Congress, Holland, 1948," pp. II-130 to II-141, North Holland Publishing Co.
25. Ostwald, Wolfgang, *Kolloid-Z.*, **36**, 99 (1925).
26. Powell, R. E., and Henry Eyring, *Nature*, **154**, 427 (1944).
27. Prandtl, Ludwig, *Reports of the Aerodyn. Versuchsanst. Gottingen*, I. Series, 136 (1921).
28. Shaver, R. G., and E. W. Merrill, *A.I.Ch.E. Journal*, **5**, 181 (1959).
29. Sieder, E. N., and C. E. Tate, *Ind. Eng. Chem.*, **28**, 1429 (1936).
30. Thomas, D. G., "Reactor Handbook," 2 ed., Vol. 2, Chap. 1, Sect. 1. 2. 4. 2., Interscience, New York (1960).
31. ———, *Paper 14-3*, 3 Annual ANS Meeting, Pittsburgh, Pennsylvania (June, 1957).
32. von Karman, Theodore, *Z. angew. Math u. Mech.*, **1**, 233 (1921).
33. Weltman, R. N., *Natl. Advisory Comm. Aeronaut. Tech. Note 3397* (Feb., 1955).

Manuscript received August 3, 1959; revision received January 27, 1960; paper accepted January 27, 1960.